Robust Control of Parallel DC–DC Buck Converters by Combining Integral-Variable-Structure and Multiple-Sliding-Surface Control Schemes

Sudip K. Mazumder, *Member, IEEE,* Ali H. Nayfeh, and Dushan Borojević, *Member, IEEE*

***Abstract*—We develop a robust controller for parallel dc–dc buck converters by combining the concepts of integral-variable-structure and multiple-sliding-surface control. The advantages of the scheme are its simplicity in design, good dynamic response, robustness, ability to nullify the bus-voltage error and the error between the load currents of the converter modules under steady-state conditions, and ability to reduce the impact of very high-frequency dynamics due to parasitics on the closed-loop system. We describe a method for determining the region of existence and stability of the sliding manifolds for such parallel converters. The results show good steady-state and dynamic responses.**

***Index Terms*—Closed-loop system, integral-variable-structure, load currents, multiple-sliding-surface control, parallel converters,**
.

I. Introduction

PARALLEL dc–dc converters are widely used in telecommunication power supplies. They operate under closed-loop feedback control to regulate the bus voltage and enable load sharing [1]. [2]. These closed-loop converters are inherently nonlinear systems. The major sources of nonlinearities are the switching nonlinearity and the interaction among the converter modules. So far, however, the analyses in this area of power electronics are based primarily on linearized averaged (small-signal) models [3]–[13]. When a nonlinear converter has solutions other than the nominal one, small-signal analyzes cannot predict the basin of attraction of the nominal solution and the dynamics of the system after the nominal solution loses stability [14]–[28]. In addition, small-signal models cannot predict the dynamics of a switching converter in a saturated region [25], [26], [28]. Obviously, linear controllers [3], [5], [7], [8], [10]–[13] designed for such systems cannot always give robust solutions and optimum performance [29]–[31].

Manuscript received February 23, 2001; revised October 29, 2001. This work was supported by the Office of Naval Research under Grant N00014-96-1-1123(MURI), ERC Shared Facilities, and the National Science Foundation under Award EEC-9731677. Recommended by Associate Editor C. K. Tse.

S. K. Mazumder is with the Power Electronics Research Center, Department of Electrical and Computer Engineering, University of Illinois, Chicago, IL 60607-7053 USA.

A. H. Nayfeh is with the Department of Engineering Science and Mechanics, Virginia Polytechnic Institute and State University, Blacksburg, VA 24061 USA (e-mail: anayfeh@vt.edu).

D. Borojević is with the Center for Power Electronics Systems, Department of Electrical and Computer Engineering, Virginia Polytechnic Institute and State University, Blacksburg, VA 24061 USA.

Publisher Item Identifier S 0885-8993(02)04637-9.

One way to extract the best performance out of a parallel-converter system is to study its dynamics based on bifurcation analysis [32]–[35]. In this approach, the stable and unstable dynamics of the system are studied as a parameter is varied. Since almost all of the converters are nonlinear and nonautonomous, we resort to nonlinear maps [23]–[28]. Based on the movement of the Floquet multipliers associated with these maps, the bifurcations are categorized as static or dynamic. The advantage of this approach is that, if the dynamics of the systems beyond the linear region are known, one can optimize the performance of the converter. The implementation of this approach is discussed in [27], [28].

Another approach, which is the topic of discussion here, is based on the design of a robust nonlinear controller that achieves global or semiglobal stability [35]–[37] of the nominal orbit in the operating region of the parallel converter. Recently, there have been many studies of the nonlinear control of standalone dc–dc converters [38]–[47], which have focussed on variable-structure controllers (VSC) [48], [49], Lyapunov-based controllers [50]–[54], feedback linearized and nonlinear H_∞ controllers [35]–[37], [55]–[57], and fuzzy logic controllers [58]–[60]. However, there are few studies on the nonlinear control of parallel dc–dc converters where, unlike the standalone converters, there is a strong interaction among the converter modules apart from the feedforward and feedback disturbances.

In [30], a fuzzy-logic compensator is proposed for the master-slave control of a parallel dc–dc converter. The controller uses a proportional-integral-derivative (PID) expert to derive the fuzzy inference rules; it shows improved robustness as compared to linear controllers. However, the control design is purely heuristic and the stability of the overall system has not been proven. In [31], a VSC has been developed for a buck converter using interleaving. However, the interleaving scheme works only for three parallel modules. Besides, this paper does not give any details regarding the existence and stability of the sliding manifolds.

In this paper, we develop integral-variable-structure control (IVSC) schemes for N parallel dc–dc buck converters. The choice of a VSC is logical for power converters because the control and plant are both discontinuous. All of the nonlinear controllers mentioned earlier [42]–[47], which are not based on VSC, have completely relied on smooth averaged models of the power converters. Therefore, the control is valid only on a reduced-order manifold [23]–[28].

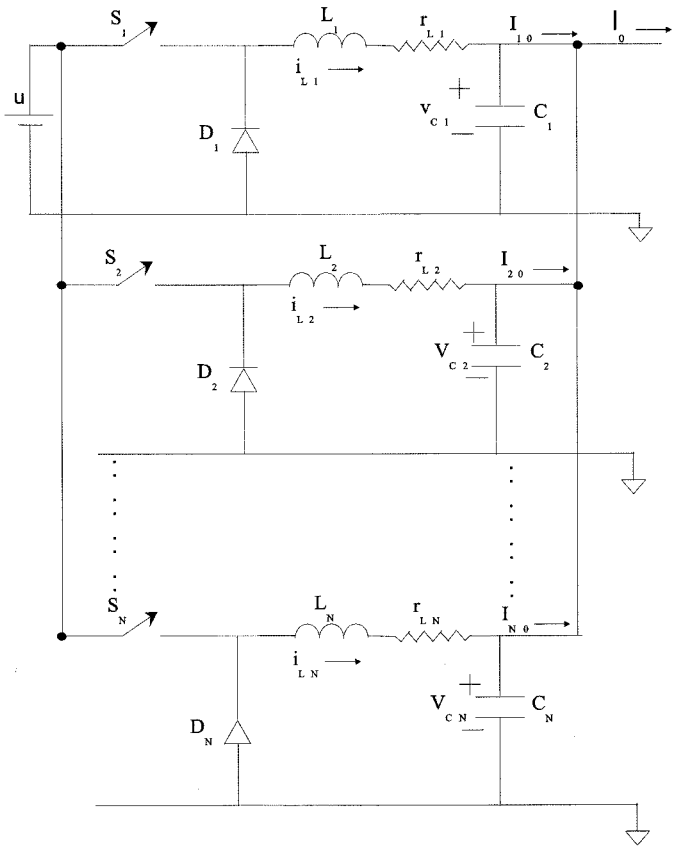

Fig. 1. Parallel dc–dc buck converter.

The IVSC retains all of the properties of a VSC; that is, simplicity in design, good dynamic response, and robustness. In addition, the integral action of the IVSC eliminates the bus-voltage error and the error between the load currents of the converter modules under steady-state conditions, and it reduces the impact of very high-frequency dynamics due to parasitics on the closed-loop system. Finally, when the error trajectories are inside the boundary layer, by modifying the control using the concepts of multiple-sliding-surface control (MSSC) [61], [62] or the block-control principle [63], [64], we are able to reject mismatched disturbances [53], [54], [65], [66] and keep the steady-state switching frequency constant. We validate our theoretical results with some relevant simulation results. We demonstrate the performance of converter modules under steady-state and transient conditions and when their parameters do not match.

II. Model of Parallel DC–DC Buck Converter

Assuming ideal switches, the dynamics of N buck converters (shown in Fig. 1) operating in parallel are governed by the following differential equations:

$$\begin{aligned}\frac{di_{L_k}}{dt} &= -\frac{1}{L_k}\left(r_{L_k}i_{L_k} + v_{C_k} - S_k u\right)\\ \frac{dv_{C_k}}{dt} &= \frac{1}{C_k}\left(i_{L_k} - I_{k_0}\right), \quad k = 1, 2, \ldots, N\end{aligned} \tag{1}$$

where the S_k are the switching functions and u represents the input voltage. The constraints on the converter model are

$$\begin{aligned}&v_{C_1} = \cdots = v_{C_N} = v_C\\ &\frac{v_C}{u} < 1\\ &\sum_{k=1}^{N} I_{k_0} = I_0\end{aligned} \tag{2}$$

where I_0 is the load current.

III. Concepts of Discontinuous Systems

The condition for the existence of the ith discontinuity surface ($\sigma_i = 0$) of a differential equation

$$\dot{y} = f(y, t, s) \tag{3}$$

with discontinuous right-hand side in the neighborhood of $\sigma_i = 0$ is [67]

$$\lim_{\sigma_i \to -0} \dot{\sigma}_i > 0 \quad \text{and} \quad \lim_{\sigma_i \to +0} \dot{\sigma}_i < 0 \quad \text{or} \quad \dot{\sigma}_i \sigma_i < 0. \tag{4}$$

If the discontinuity surface exists globally, then all of the solutions of (3) in the continuity region reach it and stay on it. For the continuity region, the definition of solution is clear [67]. However, the definition of a solution (almost everywhere) as an absolutely continuous function satisfying (4) is not always applicable for equations whose right-hand sides are discontinuous on an arbitrary smooth surface. Using the Lebesgue measure, one can apply the definition to the case in which the solutions approach the discontinuity surface on one side and leave it on the other side. When the solutions approach a discontinuity surface on both sides, the conventional definition is unsuitable because there is no indication of how a solution that has reached the discontinuity surface may continue.

Filippov [67] defined a solution for the vector differential equation

$$\dot{y} = f(y, t, s, (y)) = h(y, t) \tag{5}$$

with discontinuous feedback $s = s(y)$, where $h : \Re^n \times \Re \to \Re^n$ is measurable and essentially locally bounded. A vector function $y(t)$, defined on the interval (t_1, t_2), is a Filippov solution of (5) if it is absolutely continuous and, for almost all $t \in (t_1, t_2)$ and for arbitrary $\delta > 0$, the vector $dy(t)/dt$ belongs to the smallest convex closed set of an n-dimensional space containing all of the values of the vector function $h(\hat{y}, t)$; where $\hat{y}$ ranges over the entire δ neighborhood of the point $y(t)$ in the space y (with t fixed) except for a set of measure $\mu M = 0$; that is

$$\frac{dy(t)}{dt} \in H(y, t) \tag{6}$$

where $H(\cdot)$ is called Filippov's differential inclusion and is defined as

$$H(y, t) \equiv \bigcap_{\delta > 0} \bigcap_{\mu M > 0} \overline{\text{co}}\, h(B(y, \delta) - M). \tag{7}$$

In (7), $\overline{\text{co}}$ denotes the convex hull of a set, μ is the Lebesgue measure, and B is a ball of radius δ centered at y. The content of Filippov's solution is that the tangent vector to a solution at a time t, where it exists, must lie in the convex closure of the limiting values of the vector field in progressively smaller neighborhoods around the solution evaluated at time t.

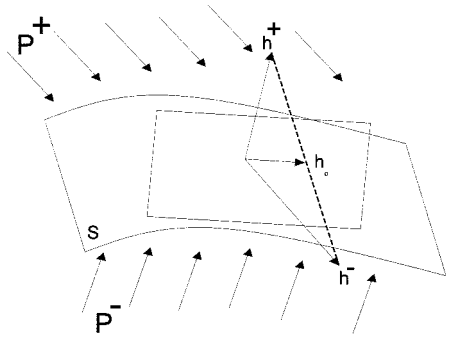

Fig. 2. Description of Filippov's solution (often called sliding motion) on a discontinuity surface S.

Let us consider a smooth surface S (shown in Fig. 2), given by $\sigma(y) = 0$, on which the function $h(y,t)$ is discontinuous. The surface S separates its neighborhood in the y space into the domains P^- and P^+. Suppose that $h(y,t)$ is bounded and, for any fixed t, its limiting values $h^+(y,t)$ and $h^-(y,t)$ exist when S is approached from P^+ and P^-. Let $h_n^+(y,t)$ and $h_n^-(y,t)$ be the projections of $h^+(y,t)$ and $h^-(y,t)$ on the normal $\bigtriangledown\sigma$ to the surface S directed toward P^+ and P^-. Then, for an absolutely continuous $y \in S$ satisfying $h_n^+(y,t) \leq 0$, $h_n^-(y,t) \geq 0$, and $h_n^-(y,t) - h_n^+(y,t) > 0$, the trajectories pointing toward S are solutions of (5) according to the differential inclusion (6) if and only if

$$\frac{dy}{dt} = \beta(t)h^+(y,t) + (1-\beta(t))h^-(y,t) = h_o(y,t) \tag{8}$$

where

$$\beta(t) = \frac{h_n^-(y,t)}{h_n^-(y,t) - h_n^+(y,t)}. \tag{9}$$

We note that the right-hand side of (8) is orthogonal to $\bigtriangledown\sigma$ and hence the solution remains on the surface S.

The sliding mode in a real-life system actually occurs not on its discontinuity surface, but within a boundary layer on which the control components may take up values different from s_i^+ and s_i^- [48], [49]. The vector $f(y,t,s)$ in (3) may, therefore, take up values which differ from those obtained with $s_i = s_i^+$ and $s_i = s_i^-$. This results in a wider convex set in the Filippov continuation method and, consequently, in a richer set of motions on the sliding mode. In order to handle the regularization problem and find feasible solutions to (3), Utkin [48] proposed an equivalent control method.

Assume that a sliding mode exits on the manifold

$$\sigma(y) = 0, \quad \sigma^T(y) = [\sigma_1(y), \sigma_2(y), \ldots, \sigma_n(y)] \tag{10}$$

which lies at the intersection of n discontinuity surfaces. Then, we can find a continuous control such that, under the initial position of the state vector on this manifold, the time derivative of the vector $\sigma(y)$ along the trajectories of system (3) is identically zero; that is

$$\dot{\sigma} = \bigtriangledown\sigma_i(y) \cdot f\left(t, y, s_1^{\text{eq}}(t,y), \ldots, s_n^{\text{eq}}(t,y)\right) = 0, \quad i = 1,2,\ldots,n. \tag{11}$$

In (11), $s^{\text{eq}}(t,y) = [s_1^{\text{eq}}(t,y), \ldots, s_n^{\text{eq}}(t,y)]$ is referred to as the equivalent control for the vector equation (3) on the sliding surface (10). Therefore, the dynamics of (3) on the sliding surface are governed by

$$\dot{y} = f[y, t, s^{\text{eq}}(y,t)]. \tag{12}$$

Thus a solution is an absolutely continuous vector-valued function, which outside the surfaces σ_i satisfies (3) and on these surfaces and on their intersections satisfies (12) for almost all t.

For a system which is linear with respect to control, when the width of the boundary layer is zero, the solutions obtained using the equivalent control method and Filippov's method are the same. The stability of the solutions of either (8) or (12) is determined using linear techniques if the sliding manifold is linear. If, however, the sliding manifold is nonlinear, then Lyapunov's first and second methods [35], [68], [69] and bifurcation analysis [32]–[35] are suitable approaches.

IV. Control Scheme

The control scheme for the converter has two modes of operation: one when the error trajectories are outside the boundary layer and the other when they are inside the boundary layer. The boundary layer, which is time-varying, is formed by a ramp signal with a frequency f_s $(=1/T)$. The limits of this boundary layer correspond to the maximum and minimum values of the ramp. At the beginning of each switching cycle, we determine whether the error trajectories (σ_k) are within the limits of the time-varying ramp and hence determine the mode of operation.

A. Control Outside the Boundary Layer

To achieve the control objectives, we use smooth hypersurfaces (sliding surfaces) defined by

$$\sigma_k = G_{k_1}\left(V_{r_k} - f_{v_k} v_{C_k}\right) + G_{k_2}\int\left(V_{r_k} - f_{v_k} v_{C_k}\right)d\tau + G_{k_3}\int\left(\frac{1}{N}\sum_{j=1}^{N} f_{i_j} i_{L_j} - f_{i_k} i_{L_k}\right)d\tau - f_{i_k} i_{L_k} \tag{13}$$

where the G_{k_1}, G_{k_2}, and G_{k_3} are the controller gains, the f_{v_k} (≤ 1) and f_{i_k} (≤ 1) are the sensor gains for the output voltages and inductor currents, and the V_{r_k} are the reference voltages for the bus. The term $(1/N)\sum_{j=1}^{N} f_{i_j} i_{L_j}$ $(= i_{L_{\text{av}}})$ represents the average of all inductor currents. While the first two terms in (13) minimize the bus voltage error, the third term enables equal sharing of power among the converter modules. The last term enhances the dynamic response of the closed-loop system.

We note that, in a conventional VSC, the integral operators in (13) are replaced with first-order derivatives. This may not be desirable for a power converter, which operates at a high switching frequency [25]. Due to its integral action, the IVSC minimizes the impact of parasitics due to a high-switching frequency. In addition, unlike a VSC, the IVSC attains steady state with reduced control effort.

Next, we differentiate (13) to obtain

$$\dot{\sigma}_k = -G_{k_1} f_{v_k} \dot{v}_{C_k} + G_{k_2}\left(V_{r_k} - f_{v_k} v_{C_k}\right) + G_{k_3}\left(\frac{1}{N}\sum_{j=1}^{N} f_{i_j} i_{L_j} - f_{i_k} i_{L_k}\right) - f_{i_k}\dot{i}_{L_k}. \tag{14}$$

Using (1), we rewrite (14) as

$$\begin{aligned}\dot{\sigma}_k = &-\frac{G_{k_1} f_{v_k}}{C_k}\left(i_{L_k} - I_{k_0}\right) + G_{k_2}\left(V_{r_k} - f_{v_k} v_{C_k}\right) \\ &+ G_{k_3}\left(\frac{1}{N}\sum_{j=1}^{N} f_{i_j} i_{L_j} - f_{i_k} i_{L_k}\right) \\ &+ \frac{f_{i_k}}{L_k}\left(r_{L_k} i_{L_k} + v_{C_k} - S_k u\right). \end{aligned} \tag{15}$$

Equation (15) shows that the sliding surfaces have independent control. The general form of $\dot{\sigma}_k$ is

$$\dot{\sigma}_k = a_k(\Psi_k) + b_k S_k + c_k I_{k_0} \tag{16}$$

where $\Psi_k = [i_{L_k} \;\; v_{C_k}]^T$ and

$$\begin{aligned} a_k = &-\frac{G_{k_1} f_{v_k}}{C_k} i_{L_k} + G_{k_2}\left(V_{r_k} - f_{v_k} v_{C_k}\right) \\ &+ G_{k_3}\left(\frac{1}{N}\sum_{j=1}^{N} f_{i_j} i_{L_j} - f_{i_k} i_{L_k}\right) \\ &+ \frac{f_{i_k}}{L_k}\left(r_{L_k} i_{L_k} + v_{C_k}\right) \\ b_k = &-\frac{f_{i_k}}{L_k} u \\ c_k = &\frac{G_{k_1} f_{v_k}}{C_k}. \end{aligned} \tag{17}$$

We define

$$S_k = \frac{1}{2}(1 + \operatorname{sign}(\sigma_k)) = S_{k_{\text{eq}}} + S_{k_n} \tag{18}$$

where $S_{k_{\text{eq}}}$ and S_{k_n} represent the equivalent control [48], [49] and the nonlinear switching control and

$$\operatorname{sign}(\sigma_k) = \begin{cases} 1, & \text{if } \sigma_k > 0 \\ -1, & \text{if } \sigma_k < 0 \end{cases}. \tag{19}$$

These two controls must satisfy the following constraints:

$$\begin{aligned} &S_k^- < S_{k_{\text{eq}}} < S_k^+ \quad (S_k^- = 0 \text{ and } S_k^+ = 1) \\ &S_k^- - S_{k_{\text{eq}}} \le S_{k_n} \le S_k^+ - S_{k_{\text{eq}}}. \end{aligned} \tag{20}$$

Knowing that b_k^{-1} exists, we equate (16) to zero, solve for $S_{k_{\text{eq}}}$, and obtain

$$S_{k_{\text{eq}}} = -b_k^{-1}\left(a_k(\Psi_k) + c_k I_{k_0}\right). \tag{21}$$

Substituting $S_{k_{\text{eq}}}$ into (18) and using (16) and (4), we obtain the following existence condition:

$$\sigma_k b_k S_{k_n} < 0. \tag{22}$$

Because $b_k < 0$, (22) is satisfied provided that

$$S_{k_n} = \begin{cases} >0, & \text{if } \sigma_k > 0 \\ <0, & \text{if } \sigma_k < 0 \end{cases} \tag{23}$$

and $S_{k_{\text{eq}}}$ satisfies (20). For example, substituting (17) into (21) yields

$$\begin{aligned} S_{k_{\text{eq}}} = &\frac{1}{u}\frac{L_k}{C_k}\frac{f_{v_k}}{f_{i_k}} G_{k_1}\left(I_{k_0} - i_{L_k}\right) + \frac{1}{u}\frac{L_k}{f_{i_k}} G_{k_2}\left(V_{r_k} - f_{v_k} v_{C_k}\right) \\ &+ \frac{1}{u}\frac{L_k}{f_{i_k}} G_{k_3}\left(\frac{1}{N}\sum_{j=1}^{N} f_{i_j} i_{L_j} - f_{i_k} i_{L_k}\right) \\ &+ \frac{1}{u}\left(r_{L_k} i_{L_k} + v_{C_k}\right). \end{aligned} \tag{24}$$

Knowing that $1/u < 1$, f_{v_k}/f_{i_k} is small, $L_k/C_k < 1$ for proper design, and the fourth term in (24) is less than one (because $r_L \approx 0$), we can make $S_{k_{\text{eq}}}$ satisfy (20) by properly chosing G_{k_1}, G_{k_2}, and G_{k_3}.

The stability of the dynamics on the sliding manifold for the parallel buck converter is straightforward because the dynamical equations describing the closed-loop system are in regular form [48], [49] on this manifold. The dynamical equations on the reduced-order manifold $\cap \sigma_k = 0 \; (k = 1, N)$ are given by

$$\begin{aligned} \dot{e}_{1_k} &= -f_{v_k}\dot{v}_{C_k} = -\frac{f_{v_k}}{C_k}\left(i_{L_k} - I_{k_0}\right) \\ \dot{e}_{2_k} &= e_{1_k} = V_{r_k} - f_{v_k} v_{C_k} \\ \dot{e}_{3_k} &= \frac{1}{N}\sum_{j=1}^{N} f_{i_j} i_{L_j} - f_{i_k} i_{L_k}. \end{aligned} \tag{25}$$

Because $\sigma_k = 0$ on the sliding surface, using (13), we obtain

$$f_{i_k} i_{L_k} = G_{k_1} e_{1_k} + G_{k_2} e_{2_k} + G_{k_3} e_{3_k}. \tag{26}$$

Substituting (26) into (25), we obtain a set of linear differential equations of the following form:

$$\begin{aligned} \dot{e}_{1_k} &= \phi_{1_k}\left(e_{1_k}, e_{2_k}, e_{3_k}\right) + \frac{f_{v_k}}{C_k} I_{k_0} \\ \dot{e}_{2_k} &= \phi_{2_k}\left(e_{1_k}\right) \\ \dot{e}_{3_k} &= \phi_{3_k}\left(e_{1_k}, e_{2_k}, e_{3_k}\right) + i_{L_{\text{av}}} \end{aligned} \tag{27}$$

where ϕ_{1_k}, ϕ_{2_k}, and ϕ_{3_k} are linear functions. For a passive load, the stability of (27) can be determined by the eigenvalues of its Jacobian. For example, if the load is a resistor of R ohm, then $I_{k_0} = v_{C_k}/R$. If I_{k_0} has a time-varying perturbation in addition to its nominal value, then the stability of the solutions of (27) can be analyzed by using either Floquet theory or the Lyapunov method [26], or simply by analyzing the state-transition matrix of (27) [69].

B. Control Inside the Boundary Layer

The derivation of the control laws in the preceding section assumes ideal sliding surfaces. In reality, the switching frequency is finite, and hence, instead of ideal sliding surfaces given by (14), we have boundary layers around them. For a boundary layer of finite width, the control laws derived in the preceding section only guarantee that the error trajectories will reach the boundary layer. Within a boundary layer/quasisliding surface, the dynamics of the system is infinite dimensional due to the delay [25]–[28]. One way to describe the dynamics of the converter within the quasisliding surfaces is through a nonlinear map [23]–[28]. In [70], we describe the digital control design using such a map for a parallel three-phase boost converter system. Another way to describe the dynamics within the quasisliding surfaces is through a state-space averaged model [23], [25] that follows from Fillipov's concept of differential inclusion. We use the latter approach in this paper.

The state-space averaged model for the parallel dc–dc buck converter is given by [71]

$$\begin{aligned} \frac{d\bar{i}_{L_k}}{dt} &= -\frac{1}{L_k}\left(r_{L_k}\bar{i}_{L_k} + \bar{v}_{C_k} - d_k u\right) \\ \frac{d\bar{v}_{C_k}}{dt} &= \frac{1}{C_k}\left(\bar{i}_{L_k} - \bar{I}_{k_0}\right), \quad k = 1, 2, \ldots, N. \end{aligned} \tag{28}$$

where d_k is the duty ratio. We make an important observation at this point. The control based on the averaged model works only inside the boundary layer. Outside the boundary layer, the

controller uses the switching model. Therefore, the controller can guarantee stability even under saturation. Conventional controllers based on small-signal models ignore the impact of saturation and other nonlinearities. For instance, the averaged model of a parallel-boost converter is nonlinear.

Next, we define the following sliding surfaces:

$$\begin{aligned}\bar{\sigma}_{1_k} &= G_{k_1}\bar{e}_{1_k} + G_{k_2}\bar{e}_{2_k} + G_{k_3}\bar{e}_{3_k}\\ \bar{\sigma}_{2_k} &= \bar{i}_{L_{kd}} - \bar{i}_{L_k}\end{aligned} \tag{29}$$

where

$$\begin{aligned}\bar{e}_{1_k} &= V_{r_k} - f_{v_k}\bar{v}_{C_k}\\ \bar{e}_{2_k} &= \int (V_{r_k} - f_{v_k}\bar{v}_{C_k})\, d\tau\end{aligned} \tag{30}$$

$$\bar{e}_{3_k} = \int \left(\frac{1}{N}\sum_{j=1}^{N} f_{i_j}\bar{i}_{L_j} - f_{i_k}\bar{i}_{L_k}\right) d\tau. \tag{31}$$

Differentiating $\bar{\sigma}_{1_k}$, we obtain

$$\dot{\bar{\sigma}}_{1_k} = G_{k_1}\dot{\bar{e}}_{1_k} + G_{k_2}\dot{\bar{e}}_{2_k} + G_{k_3}\dot{\bar{e}}_{3_k}. \tag{32}$$

Substituting (28) into (31) yields

$$\dot{\bar{\sigma}}_{1_k} = -\frac{G_{k_1}f_{v_k}}{C_k}\left(\bar{i}_{L_k} - \bar{I}_{k_0}\right) + G_{k_2}\dot{\bar{e}}_{2_k} + G_{k_3}\dot{\bar{e}}_{3_k}. \tag{33}$$

Substituting for $\bar{i}_{L_k}$ from (29) into (32), we obtain

$$\dot{\bar{\sigma}}_{1_k} = \frac{G_{k_1}f_{v_k}}{C_k}\left(\bar{I}_{k_0} + \bar{\sigma}_{2_k} - \bar{i}_{L_{kd}}\right) + G_{k_2}\dot{\bar{e}}_{2_k} + G_{k_3}\dot{\bar{e}}_{3_k}. \tag{34}$$

We let

$$\bar{i}_{L_{kd}} = \beta_{1_k}\bar{\sigma}_{1_k} + \beta_{2_k}\,\mathrm{sign}\,(\bar{\sigma}_{1_k}) + \beta_{3_k}\dot{\bar{e}}_{2_k} + \beta_{4_k}\dot{\bar{e}}_{3_k} \tag{35}$$

where β_{1_k}, β_{2_k}, β_{3_k}, and β_{4_k} are constants, in (33) and obtain

$$\begin{aligned}\dot{\bar{\sigma}}_{1_k} = &-\frac{G_{k_1}f_{v_k}}{C_k}\left(\beta_{1_k}\bar{\sigma}_{1_k} + \beta_{2_k}\,\mathrm{sign}\,(\bar{\sigma}_{1_k}) - \bar{I}_{k_0} - \bar{\sigma}_{2_k}\right)\\ &-\left(\frac{G_{k_1}f_{v_k}\beta_{3_k}}{C_k} - G_{k_2}\right)\dot{\bar{e}}_{2_k}\\ &-\left(\frac{G_{k_1}f_{v_k}\beta_{4_k}}{C_k} - G_{k_3}\right)\dot{\bar{e}}_{3_k}.\end{aligned} \tag{36}$$

Next, we choose $\beta_{3_k} = (C_k G_{k_2})/(f_{v_k} G_{k_1})$ and $\beta_{4_k} = (C_k G_{k_3})/(f_{v_k} G_{k_1})$ and reduce (35) to

$$\dot{\bar{\sigma}}_{1_k} = -\frac{G_{k_1}f_{v_k}}{C_k}\left(\beta_{1_k}\bar{\sigma}_{1_k} + \beta_{2_k}\,\mathrm{sign}\,(\bar{\sigma}_{1_k}) - \bar{I}_{k_0} - \bar{\sigma}_{2_k}\right) \tag{37}$$

Equation (37) shows that, when $\bar{\sigma}_{2_k} = 0$, the dynamics on $\bar{\sigma}_{1_k} = 0$ are convergent (for $\bar{\sigma}_{1_k} > 0$ or $\bar{\sigma}_{1_k} < 0$) provided that $\beta_{2_k} > \bar{I}_{k_0\max}$. We assume that $\bar{\sigma}_{2_k} = 0$ and design the control such that the the rate of convergence of the dynamics on $\bar{\sigma}_{2_k} = 0$ are much faster than those on $\bar{\sigma}_{1_k} = 0$.

Next, we differentiate $\bar{\sigma}_{2_k}$ in (29) and set it equal to $-(\alpha_{1_k}/L_k)\sigma_{2_k}$ (where α_{1_k} is a positive constant) to guarantee convergence of the dynamics on $\bar{\sigma}_{2_k} = 0$; the result is

$$\begin{aligned}\dot{\bar{\sigma}}_{2_k} &= \dot{\bar{i}}_{L_{kd}} - \dot{\bar{i}}_{L_k} = \dot{\bar{i}}_{L_{kd}} + \frac{r_{L_k}}{L_k}\bar{i}_{L_k} + \frac{1}{L_k}\bar{v}_{C_k} - \frac{1}{L_k}d_k u\\ &= -\frac{\alpha_{1_k}}{L_k}\bar{\sigma}_{2_k}.\end{aligned} \tag{38}$$

Next, using the Lyapunov function

$$V(\bar{\sigma}_{1_k}, \bar{\sigma}_{2_k}) = \frac{1}{2}\left(\bar{\sigma}_{1_k}^2 + \bar{\sigma}_{2_k}^2\right) \tag{39}$$

and (37) and (38), we can show that

$$\begin{aligned}\dot{V} &= \bar{\sigma}_{1_k}\dot{\bar{\sigma}}_{1_k} + \bar{\sigma}_{2_k}\dot{\bar{\sigma}}_{2_k}\\ &= \bar{\sigma}_{1_k}\left(-\frac{G_{k_1}f_{v_k}}{C_k}\left(\beta_{1_k}\bar{\sigma}_{1_k} + \beta_{2_k}\,\mathrm{sign}\,(\bar{\sigma}_{1_k})\right.\right.\\ &\quad\left.\left. - \bar{I}_{k_0} - \bar{\sigma}_{2_k}\right)\right) + \bar{\sigma}_{2_k}\left(-\frac{\alpha_{1_k}}{L_k}\bar{\sigma}_{2_k}\right)\\ &\le -\left(\frac{G_{k_1}f_{v_k}}{C_k}\beta_{1_k}\bar{\sigma}_{1_k}^2 + \frac{\alpha_{1_k}}{L_k}\bar{\sigma}_{2_k}^2\right) + \frac{G_{k_1}f_{v_k}}{C_k}\bar{\sigma}_{1_k}\bar{\sigma}_{2_k}\\ &= -\left(\sqrt{\frac{G_{k_1}f_{v_k}}{C_k}\beta_{1_k}}\,\bar{\sigma}_{1_k} - \frac{1}{2}\sqrt{\frac{G_{k_1}f_{v_k}}{C_k\beta_{1k}}}\,\bar{\sigma}_{2_k}\right)^2\\ &\quad -\left(\frac{\alpha_{1_k}}{L_k} - \frac{1}{4}\frac{G_{k_1}f_{v_k}}{C_k\beta_{1k}}\right)\bar{\sigma}_{2_k}^2\end{aligned} \tag{40}$$

is less than zero provided that $(\alpha_{1_k}C_k\beta_{1_k})/(L_k G_{k_1} f_{v_k}) > (1/4)$..

From (38), we obtain

$$d_k = \frac{1}{u}\left(\alpha_{1_k}\sigma_{2_k} + L_k\dot{\bar{i}}_{L_{kd}} + r_{L_k}\bar{i}_{L_k} + \bar{v}_{C_k}\right). \tag{41}$$

Using this duty ratio and a ramp signal (with fixed frequency), we can operate N parallel converters in synchronicty or interleaving. The main difficulty in implementing (41) is calculating $\dot{\bar{i}}_{L_{kd}}$. Green and Hedrick [61] solved this problem approximately by using the first principle of calculus and obtained

$$\dot{\bar{i}}_{L_{kd}} = \frac{\bar{i}_{L_{kd}}(n+1) - \bar{i}_{L_{kd}}(n)}{T}. \tag{42}$$

A better approach was proposed by Gerdes [72] and Swaroop [62] using the concept of a linear filter. With this approach, we make a minor change in our control derivation. First, we define an auxiliary variable $\underline{i}_{L_k}$ and then pass it through the linear filter

$$\tau_f\dot{\bar{i}}_{L_{kd}} + \bar{i}_{L_{kd}} = \underline{i}_{L_k}, \quad \bar{i}_{L_{kd}}(0) = \underline{i}_{L_{kd}}(0) \tag{43}$$

to obtain $\dot{\bar{i}}_{L_{kd}}$. In (43), τ_f is a positive constant, which should be chosen large enought to reduce the high-frequency component of $\underline{i}_{L_k}$, but small enough so as not to alter the low-frequency component which is, in fact, the equivalent control that we need [73]. Finally, we substitute $\underline{i}_{L_k}$ for $\bar{i}_{L_k}$ in (35) and obtain

$$\underline{i}_{L_{kd}} = \beta_{1_k}\bar{\sigma}_{1_k} + \beta_{2_k}\,\mathrm{sign}\,(\bar{\sigma}_{1_k}) + \beta_{3_k}\dot{\bar{e}}_{2_k} + \beta_{4_k}\dot{\bar{e}}_{3_k}. \tag{44}$$

This solves the control problem inside the limits of the boundary layer.

The implementation of the overall control scheme described in this section and in Section IV-B can be analog or digital. At the beginning of each switching cycle, by determining whether the σ_k are outside or inside the limits of the boundary layer, we implement the control described in either Section IV-A or in this section. To avoid the possibility of a border collision [18], [25], we use comparators with a small hysterisis.

V. Results

We performed several simulations on a parallel-buck converter that has two modules (M1 and M2), the nominal values of their parameters are shown in Table I. The input voltage varies between 25–50 V. The output voltage is regulated at 5 V. The objective of the simulations is to find out the effectiveness of the sliding-mode control schemes in regulating the bus voltage and sharing the power delivered to a resistive load under steady-state

TABLE I
NOMINAL PARAMETERS FOR M1 AND M2

Parameter	Nominal Value
$r_{L_1} = r_{L_2} = r_{L_n}$	0.021 Ω
$L_1 = L_2 = L_n$	50 μH
$C_1 = C_2 = C_n$	4400 μF
$V_{r_1} = V_{r_2}$	2.0 V
$f_{i_1} = f_{i_2} = f_{i_n}$	1.0
$f_{v_1} = f_{v_2} = f_{v_n}$	0.4
$G_{1_1} = G_{2_1} = G_{n_1}$	$2*10^2$
$G_{1_2} = G_{2_2} = G_{n_2}$	$10*10^4$
$G_{1_3} = G_{2_3} = G_{n_3}$	$5*10^2$
Switching frequency	$100kHz$
DC offset of ramps	1.8 V
Height of ramps	3.0 V

and dynamic conditions. The controller parameters are tuned so that, for the worst disturbances, the conditions of existence of the sliding modes are satisfied and the dynamics on the sliding manifold are stable as per (27). Because it is physically impossible to have identical converters and an infinite switching frequency, we demonstrate the transient and steady-state performance of the control to variations in the parameters of the two modules under a finite switching frequency. To obtain a finite switching frequency inside the boundary layer, we compare the error signals of each module obtained using d_k with ramp signals having a switching frequency of 100 kHz. For operating the modules using interleaving, we phase shift the ramp signals of the two modules by one-half of a switching-cycle period.

Fig. 3 shows the response of the closed-loop converter when it is subjected to a sudden change in the load resistance from 2.5 Ω to 0.625 Ω, which is the maximum variation in load allowed for the given converter. The input voltage is fixed at its minimum (i.e., 25 V), and hence M1 and M2 are subjected to the worst transient load. We consider two cases: one when M1 and M2 are identical and the other when they are different. The results for case one are shown in Fig. 3(a)–(c). They show that the drop in the output voltage is less than 1% even though the load resistance is decreased four-fold. Besides, sharing of the power delivered to the load is good under steady-state and transient conditions.

Although the responses of the converter for case one are good, in real life, due to manufacturing tolerances, it is not possible to have identical modules. Therefore, the second case considers a more practical scenario. We fix $L_1, C_1, G_{1_1}, G_{1_2}$, and G_{1_3} at their nominal values but change the parameters for M2 so that $L_2 = 0.75L_n, C_2 = 0.75C_n, G_{2_1} = 0.9G_{n_1}, G_{2_2} = 0.9G_{n_2}$, and $G_{2_3} = 0.9\,G_{n_3}$. These parametric variations are more than what one will typically encounter for such converters [74]. The results in Fig. 3(d)–(f) show that, inspite of the parametric variations, the transient and steady-state performances of the converter are close to the ideal case.

In the second case, we investigate whether M1 and M2 can operate with interleaving. A closer examination of the inductor

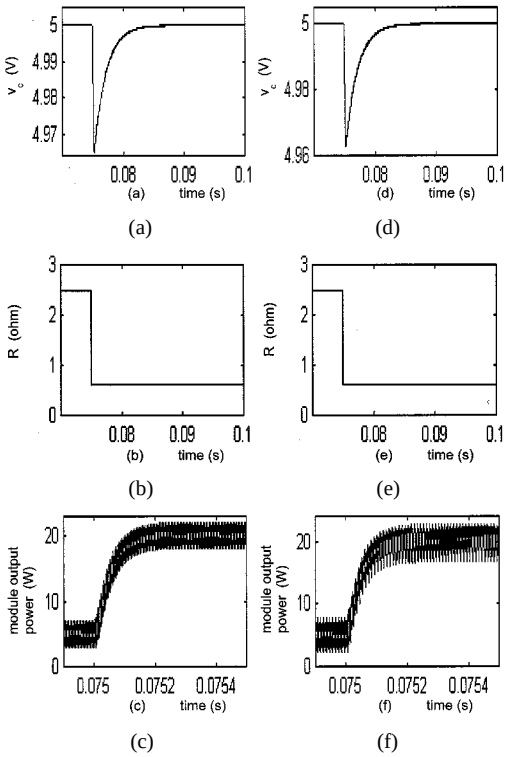

Fig. 3. Dynamic and steady-state performance of a parallel-buck converter when the parameters of the two modules are the same (a)–(c) and when they are different (d)–(f). The converter is initially in steady state and then subjected to a sudden change in the load resistance.

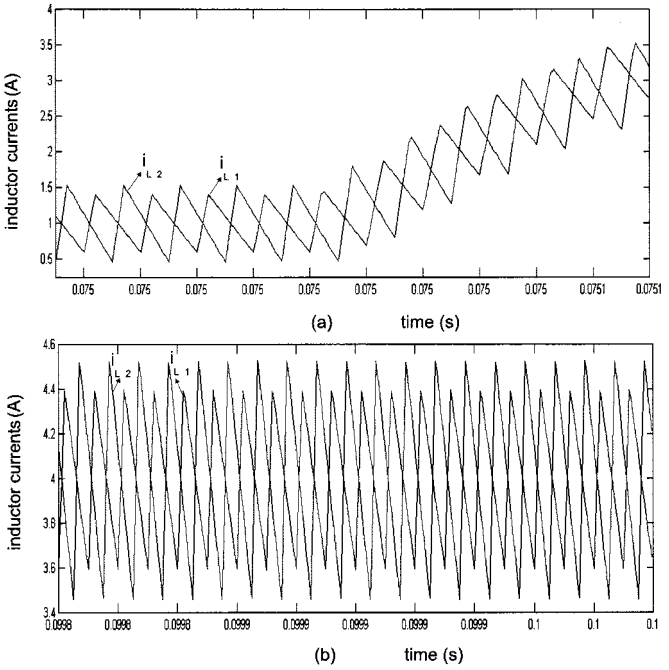

Fig. 4. Waveforms of the inductor currents i_{L_1} and i_{L_2} are phase-shifted by half the switching-cycle period. Thus, the new variable-structure controller ensures interleaved/phase-shifted operation during (a) transient and (b) steady-state conditions and keeps the switching frequency constant.

currents in Fig. 4(a)–(b) under steady-state and transient conditions show that indeed they operate with a phase shift of one-half of the switching-cycle period. The ripple of the current i_{L_2} is larger than that of i_{L_1} because the magnitude of L_2 is smaller

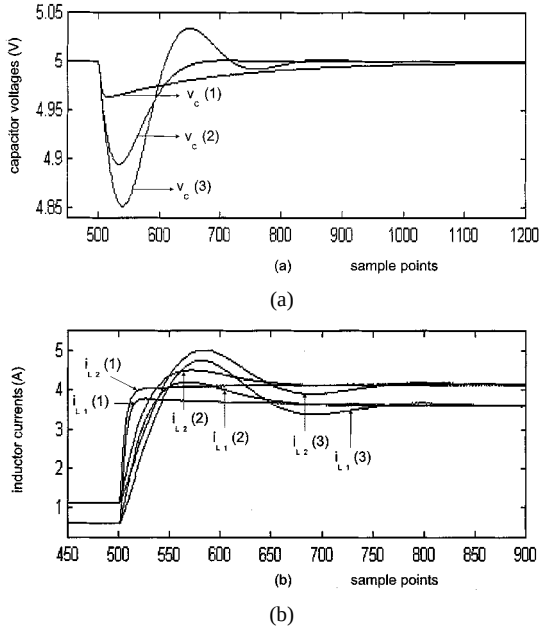

Fig. 5. Impact of variations in the controller gains G_{1_1} and G_{2_1} on the (a) output voltages and (b) the inductor currents of M1 and M2.

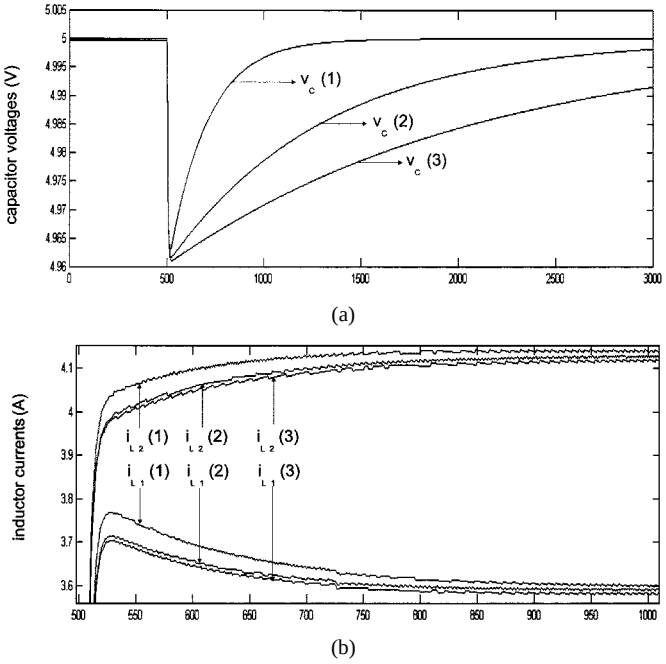

Fig. 6. Effect of variations in the controller gains G_{1_2} and G_{2_2} on the (a) output voltages and (b) the inductor currents of the parallel converter.

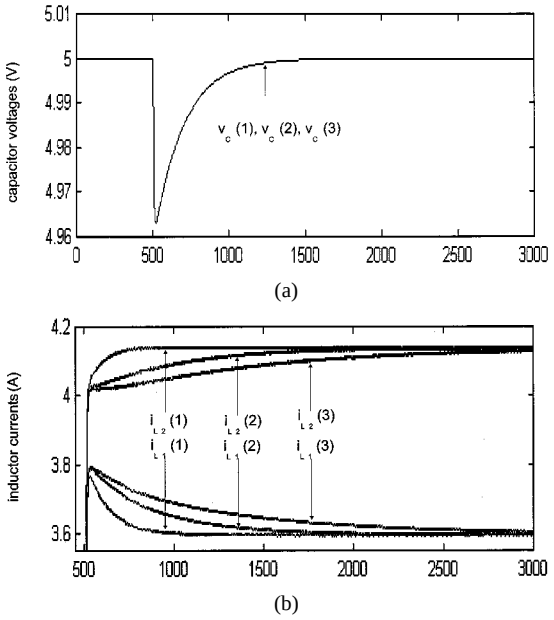

Fig. 7. Impact of variations in the controller gains G_{1_3} and G_{2_3} on the (a) output voltages and (b) the inductor currents of the converter modules.

than that of L_1. The interleaved operation of the converter is possible because, inside the boundary layer, the controllers use the duty-ratio signals for pulse-width modulation. The latter ensures the operation of the converter with a constant switching frequency. We note that, using a conventional sliding-mode control, interleaving and constant frequency of operation are not possible [49].

The choice of the controller gains $G_{1_1}, G_{2_1}, G_{1_2}, G_{2_2}, G_{1_3}$, and G_{2_3} is critical to the steady-state and transient responses of the closed-loop converter. In Figs. 5–7, we show the impact of variations in these controller gains on the performance of the converter for the second case. We fix the input voltage at 25 V and change the load resistance from 2.5 Ω to 0.625 Ω. We sampled the inductor currents and the capacitor voltages at the switching frequency to suppress the ripple from the waveforms and obtain a clearer comparison. The sampling is done at the beginning of each switching cycle of M1. At this instant and under steady-state conditions, i_{L_1} attains its lowest value. Because M2 operates with a phase shift of one-half of a switching cycle as compared to M1, the sampled value of i_{L_2} will in general be larger than that of i_{L_1} at the sampling instant.

Fig. 5(a) and (b) show the effect of variations in G_{1_1} and G_{2_1} on the output voltages and inductor currents. The plots marked $v_C(1)$, $i_{L_1}(1)$, and $i_{L_2}(1)$ are obtained using $G_{1_1} = G_{n_1}$ and $G_{2_1} = 0.9G_{n_1}$ with the remaining parameters being the same as in case two. The other sets of plots marked $v_C(2)$, $i_{L_1}(2)$, and $i_{L_2}(2)$, and $v_C(3)$, $i_{L_1}(3)$, and $i_{L_2}(3)$ are obtained by reducing only G_{1_1} and G_{2_1} by 50% and 75%, respectively. When G_{1_1} and G_{2_1} are reduced, the transient response of the system deteriorates. This is prominent in the plots marked $v_C(3)$, $i_{L_1}(3)$, and $i_{L_2}(3)$ of Fig. 5, which show a strong undershoot and an overshoot.

Next, we show in Fig. 6(a) and (b) the effect of variations in G_{1_2} and G_{2_2}. Initially, the values of all of the parameters of M1 and M2 are the same as those in case two. The waveforms for this case are marked $v_C(1), i_{L_1}(1)$, and $i_{L_2}(1)$. Then, we reduce G_{1_2} and G_{2_2} by 50% and 75%. The results for these three cases are denoted by $v_C(2)$, $i_{L_1}(2)$, and $i_{L_2}(2)$, and $v_C(3)$, $i_{L_1}(3)$, and $i_{L_2}(3)$, respectively. The results show that, as G_{1_2} and G_{2_2} are reduced, the capacitor voltage takes much longer to attain a steady state immediately after a transient. On the other hand, increasing G_{1_2} and G_{2_2} too much results in an overshoot of the inductor currents. The trade-off in the gains depends on the application of the power supply.

Similarly, by swapping G_{1_3} for G_{1_2} and G_{2_3} for G_{2_2}, we obtain Fig. 7(a) and (b), which show the impact of these controller gains on the load sharing. The corresponding plots are

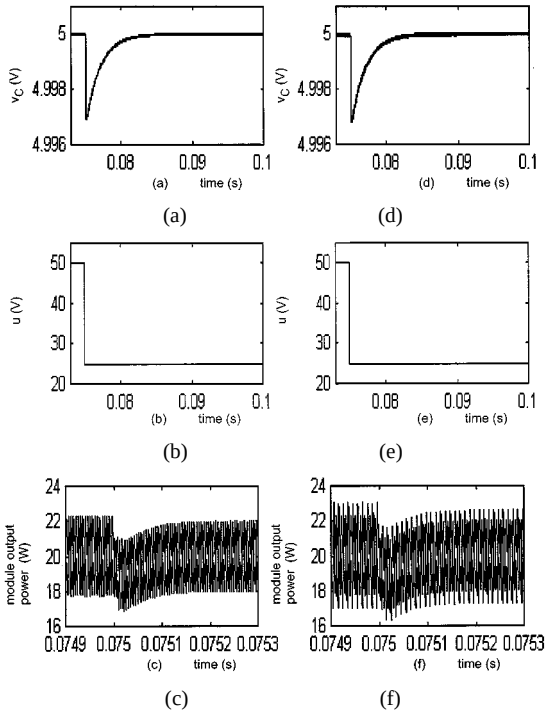

Fig. 8. Transient and steady-state performance of a parallel-buck converter when the parameters of the two modules are the same (a)–(c) and when they are different (d)–(f). The converter is initially in steady state and then subjected to a sudden change in the input voltage.

marked $v_C(1)$, $i_{L_1}(1)$, and $i_{L_2}(1)$, $v_C(2)$, $i_{L_1}(2)$, and $i_{L_2}(2)$, and $v_C(3)$, $i_{L_1}(3)$, and $i_{L_2}(3)$, respectively. First, we observe that the effect of the variations in G_{1_3} and G_{2_3} on the output voltage is negligible. Second, with a reduction in the gains, the load sharing deteriorates immediately after the transient condition. Hence, G_{1_3} and G_{2_3} must be chosen carefully; otherwise an uneven distribution of power among the converter modules occurs.

Finally, we demonstrate the responses of the parallel converter when the input voltage changes from 50 V to 25 V. This variation in the input voltage is the maximum allowed by the design specifications. The load resistance is fixed at its minimum (i.e., 0.625 Ω), and hence M1 and M2 are subjected to the worst transient input voltage. We again consider the same two cases used to obtain Fig. 3(a)–(f). Fig. 8(a)–(c) and (d)–(f) show the results for cases one and two, respectively. They show that the drop in the output voltage is less than 1%. In addition, interleaving between the two converter modules, for the ideal and realistic cases, is maintained under static and dynamic conditions. It is obvious that, even under a severe feedforward disturbance, the performance of the converter is good.

VI. Conclusion

We describe a robust control scheme for parallel dc–dc buck converters and determine the region of existence of the sliding surfaces and the stability of the reduced-order dynamical system on the sliding manifold. The control scheme combines the concepts of integral-variable-structure- and multiple-sliding-surface control and has several advantages.

1) First, it is easy to design because each sliding surface is independently controlled. As such, the operation of a parallel converter with N modules is not hampered even if a module fails.
2) Second, the controller yields good transient responses even under parametric variations.
3) Third, the controller eliminates the bus-voltage error and the error between the line currents of the converter modules under steady-state conditions. This is achieved with a reduced control effort due to the integral action of the controller.
4) Fourth, the integrators in the control scheme can reduce the impact of very high-frequency dynamics due to parasitics on an experimental closed-loop system.
5) Fifth, the control scheme within the boundary layer enables operation of the converter with a finite switching frequency.
6) Sixth, the converter modules can be operated in interleaving or synchronicity modes.
7) Finally, the control scheme can also be applied to nonminimum-phase converters.

In a follow up paper, we will publish the results on the performance of a parallel-boost converter, which uses such a control scheme.

References

[1] M. Jordan, "Load share IC simplifies power supply design," in *Proc. High Freq. Power Conv. Conf.*, 1991, pp. 65–76.
[2] ——, UC3907 load share IC simplifies parallel power supply design, in Unitrode Applicat. Note, vol. U-129, 1991.
[3] T. Kohama, T. Ninomiya, M. Shoyama, and F. Ihara, "Dynamic analysis of parallel-module converter system with current balance controllers," in *Proc. IEEE Int. Telecomm. Energy Conf.*, 1994, pp. 190–195.
[4] V. J. Thottuvelil and G. C. Verghese, "Stability analysis of paralleled dc–dc converters with active current sharing," in *Proc. IEEE Power Electron. Spec. Conf.*, 1996, pp. 1080–1086.
[5] K. Siri, C. Q. Lee, and T. F. Wu, "Current distribution control for parallel-connected converters," *IEEE Trans. Aerosp. Electron. Syst.*, vol. 28, no. 3, pp. 829–850, 1992.
[6] Q. Chen, "Stability analysis of paralleled rectifier systems," in *Proc. IEEE Int. Telecomm. Energy Conf.*, 1995, pp. 35–40.
[7] J. Rajagopalan, K. Xing, Y. Guo, and F. C. Lee, "Modeling and dynamic analysis of paralleled dc–dc converters with master/slave current sharing control," in *Proc. IEEE Appl. Power Electron. Conf.*, 1996, pp. 678–684.
[8] Y. Panov, J. Rajagopalan, and F. C. Lee, "Analysis and design of N paralleled dc–dc converters with master-slave current sharing control," in *Proc. IEEE Appl. Power Electron. Conf.*, 1996, pp. 678–684.
[9] D. S. Garabandic and T. B. Petrovic, "Modeling parallel operating PWM dc–dc power supplies," *IEEE Trans. Ind. Electron.*, vol. 42, pp. 545–550, Oct. 1995.
[10] V. J. Thottuvelil and G. C. Verghese, "Analysis and control design of paralleled dc/dc converters with current sharing," *IEEE Trans. Power Electron.*, vol. 13, pp. 635–644, July 1998.
[11] K. Siri, C. Q. Lee, and T.-F. Wu, "Current distribution control for parallel connected converters: I," *IEEE Trans. Aerosp. Electron. Syst.*, vol. 28, pp. 829–840, 1992.
[12] ——, "Current distribution control for parallel connected converters: II," *IEEE Trans. Aerosp. Electron. Syst.*, vol. 28, pp. 841–851, Mar. 1992.
[13] I. Batarseh, K. Siri, and H. Lee, "Investigation of the output droop characteristics of parallel-connnected dc–dc converters," in *Proc. IEEE Power Electron. Spec. Conf.*, vol. 1, 1994, pp. 1342–1351.
[14] J. R. Wood, "Chaos: A real phenomenon in power electronics," in *Proc. IEEE Appl. Power Electron. Conf. Expo.*, 1989, pp. 115–124.
[15] D. C. Hamill and J. H. B. Deane, "Modeling of chaotic dc–dc converters by iterated nonlinear mappings," *IEEE Trans. Power Electron.*, vol. 7, pp. 25–36, Jan. 1992.

[16] E. Fossas and G. Olivar, "Study of chaos in the buck converter," *IEEE Trans. Circuits Syst.*, vol. 43, pp. 13–25, Jan. 1996.

[17] C. K. Tse, "Flip bifurcation and chaos in three-state boost switching regulators," *IEEE Trans. Circuits Syst.*, vol. 41, pp. 16–23, Jan. 1994.

[18] S. Banerjee, E. Ott, J. A. Yorke, and G. H. Yuan, "Anomalous bifurcations in dc–dc converters: Borderline collisions in piecewise smooth maps," in *Proc. IEEE Power Electron. Spec. Conf.*, 1997, pp. 1337–1344.

[19] I. Zafrany and B. Yaakov, "A chaos model of subharmonic oscillations in current mode PWM boost converters," in *Proc. IEEE Power Electron. Spec. Conf.*, 1995, pp. 1111–1117.

[20] R. W. Erickson, S. Ćuk, and R. D. Middlebrook, "Large-signal modeling and analysis of switching regulators," in *IEEE Power Electron. Spec. Conf.*, 1982, pp. 240–250.

[21] D. M. Wolf, M. Verghese, and S. R. Sanders, "Bifurcation of power electronic circuits," *J. Franklin Inst.*, pp. 957–999, 1994.

[22] S. Chandrasekaran, "Optimization tools for subsystem design in aircraft power distribution systems," Ph.D. dissertation, Dept. of Elect. & Comput. Eng., Virginia Polytech. Inst. and State Univ., Blacksburg, 2000.

[23] M. Alfayyoummi, A. H. Nayfeh, and D. Boroyevich, "Modeling and analysis of switching-mode dc–dc regulators," *Int. J. Bifurc. Chaos*, vol. 10, no. 2, pp. 373–390, 2000.

[24] ——, "Input filter interactions in dc–dc switching regulators," in *Proc. IEEE Power Electron. Spec. Conf.*, 1999, pp. 926–932.

[25] S. K. Mazumder, A. H. Nayfeh, and D. Boroyevich, "A theoretical and experimental investigation of the fast- and slow-scale instabilities of a dc–dc converter," *IEEE Trans. Power Electron.*, vol. 16, pp. 201–216, Mar. 2001.

[26] ——, "A novel approach to the stability analysis of boost power-factor-correction circuits," in *Proc. IEEE Power Electron. Spec. Conf.*, 2001, pp. 1719–1724.

[27] ——, "Nonlinear dynamics and stability analysis of parallel dc–dc converters," in *Proc. IEEE Power Electron. Spec. Conf.*, 2001, pp. 1283–1288.

[28] ——, "A nonlinear approach to the analysis of stability and dynamics of standalone and parallel dc–dc converters," in *Proc. IEEE Appl. Power Electron. Conf.*, 2001, pp. 784–790.

[29] ——, "Development of integral-variable-structure control schemes for parallel-buck and parallel-boost dc–dc converters," in *Proc. IEEE Int. Telecommun. Energy Conf.*, 2000, pp. 82–89.

[30] B. Tomescu and H. F. VanLandingham, "Improved large-signal performance of paralleled dc–dc converters current sharing using fuzzy logic control," *IEEE Trans. Power Electron.*, vol. 14, pp. 573–577, May 1999.

[31] M. López, L. G. de Vicuña, M. Castilla, O. López, and J. Majó, "Interleaving of parallel dc–dc converters using sliding mode control," *Proc. IEEE Ind. Electron. Soc.*, vol. 2, pp. 1055–1059, 1998.

[32] A. H. Nayfeh and B. Balachandran, *Applied Nonlinear Dynamics*. New York: Wiley, 1995.

[33] I. A. Kuznetsov, *Elements of Applied Bifurcation Theory*. New York: Springer-Verlag, 1998.

[34] S. Wiggins, *Introduction to Applied Nonlinear Dynamical Systems and Chaos*. New York: Springer-Verlag, 1990.

[35] S. Sastry, *Nonlinear Systems: Analysis, Stability, and Control*. New York: Springer-Verlag, 1999.

[36] A. Isidori, *Nonlinear Control Systems*. New York: Springer-Verlag, 1995.

[37] R. Marino and P. Tomei, *Nonlinear Control Design: Geometric, Adaptive, and Robust*. New York: Simon and Schuster, 1995.

[38] H. Sira-Ramirez, G. Escobar, and R. Ortega, "On passivity-based sliding mode control of switched dc-to-dc power converters," in *Proc. IEEE Conf. Decision Contr.*, vol. 3, 1996, pp. 2525–2526.

[39] M. Rios-Bolívar, A. S. I. Zinober, and H. Sira Ramírez, "Dynamical sliding mode control via adaptive input-output linearization: A backstepping approach," in *Lecture Notes in Control and Information Sciences: Robust Control Via Variable Structure and Lyapunov Techniques*. New York: Springer-Verlag, 1996.

[40] S. R. Sanders and G. C. Verghese, "Lyapunov-based control for switching power converters," in *Proc. IEEE Power Electron. Spec. Conf.*, 1990, pp. 51–58.

[41] M. I. Angulo-Nunez and H. Sira-Ramirez, "Flatness in the passivity based control of dc-to-dc power converters," in *IEEE Conf. Decision Contr.*, vol. 4, 1998, pp. 4115–4120.

[42] A. M. Stankovic, D. J. Perreault, and K. Sato, "Synthesis of dissipative nonlinear controllers for series resonant dc–dc converters," *IEEE Trans. Power Electron.*, vol. 14, pp. 673–682, July 1999.

[43] M. Rios-Bolivar, H. Sira-Ramirez, and A. S. I. Zinober, "Output tracking control via adaptive input-output linearization: A backstepping approach," in *Proc. IEEE Conf. Decision Contr.*, vol. 2, 1995, pp. 1579–1584.

[44] A. Kugi and K. Schlacher, "Nonlinear H_∞-controller design for a dc–dc power converter," *IEEE Trans. Contr. Syst. Technol.*, vol. 7, pp. 230–237, Mar. 1999.

[45] P. Mattavelli, L. Rossetto, G. Spiazzi, and P. Tenti, "General-purpose fuzzy controller for dc/dc converters," in *Proc. IEEE Power Electron. Spec. Conf.*, 1995, pp. 723–730.

[46] F. Ueno, T. Inoue, I. Oota, and M. Sasaki, "Regulation of Cuk converters using fuzzy controllers," in *Proc. IEEE Int. Telecommun. Energy Conf.*, 1991, pp. 261–267.

[47] M. Scheffer, A. Bellini, R. Rovatti, A. Zafarana, and C. Diazzi, "A fuzzy analog controller for high performance microprocessor power supply," in *Proc. EUFIT'96 Conf.*, 1996.

[48] V. I. Utkin, *Sliding Modes in Control Optimization*. New York: Springer-Verlag, 1992.

[49] V. I. Utkin, J. Guldnerm, and J. Shi, *Sliding Mode Control in Electromechanical Systems*. New York: Taylor & Francis, 1999.

[50] P. V. Kokotovic, "The joy of feedback: Nonlinear and adaptive," *IEEE Control Syst. Mag.*, vol. 12, pp. 7–17, Mar. 1992.

[51] K. Miroslav, I. Kanellakopoulos, and P. V. Kokotovic, *Nonlinear and Adaptive Control Design*. New York: Wiley, 1995.

[52] R. A. Freeman and P. V. Kokotović, *Robust Nonlinear Control Design: State-Space and Lyapunov Techniques*. Boston, MA: Birkhäuser, 1996.

[53] S. Gutman, "Uncertain dynamical systems—A Lyapunov min-max approach," *IEEE Trans. Automat. Contr.*, vol. 24, pp. 437–443, 1979.

[54] Z. Qu, *Robust Control of Nonlinear Uncertain Systems*. New York: Wiley, 1998.

[55] J. Ball and J. W. Helton, "Factorizaion of nonlinear systems: Toward a theory for nonlinear H_∞ control," in *Proc. IEEE Conf. Decision Contr.*, vol. 3, 1988, pp. 2376–2381.

[56] H. J. William, *Extending H_∞ Control to Nonlinear Systems: Control of Nonlinear Systems to Achieve Performance Objectives*. New York: SIAM, 1999.

[57] A. J. van der Schaft, *L_2-Gain and Passivity Techniques in Nonlinear Control*. New York: Springer-Verlag, 1996.

[58] M. M. Gupta and T. Yamakawa, Eds., *Fuzzy Computing: Theory, Hardware, and Applications*. New York: Elsevier, 1988.

[59] M. Jamshidi, A. Titli, L. Zadeh, and S. Boverie, *Applications of Fuzzy Logic: Toward High Machine Intelligency Quotient Systems*. Englewood Cliffs, NJ: Prentice-Hall, 1997.

[60] G. Langholz and A. Kandel, Eds., *Fuzzy Control Systems*. Orlando, FL: CRC, 1993.

[61] J. H. Green and K. Hedrick, "Nonlinear speed control of automative engines," in *Proc. IEEE Amer. Contr. Conf.*, 1990, pp. 2891–2897.

[62] D. Swaroop, J. C. Gerdes, P. P. Yip, and J. K. Hedrick, "Dynamic surfce control of nonlinear system," in *Proc. IEEE Amer. Contr. Conf.*, 1990, pp. 3028–3034.

[63] S. V. Drakunov, D. B. Izosimov, A. G. Lukajanov, V. Utkin, and V. I. Utkin, "Block control principle: Part I," *Automat. Remote Contr.*, vol. 51, no. 5, pp. 38–46, 1990.

[64] ——, "Block control principle: Part II," *Automat. Remote Contr.*, vol. 51, no. 6, pp. 20–31, 1990.

[65] B. R. Barmish and G. Leitmann, "On ultimate boundedness control of uncertain systems in the absence of matching assuptions," *IEEE Trans. Automat. Contr.*, vol. AC-27, pp. 153–158, Jan. 1982.

[66] M. Corless and G. Leitmann, "Continuous state feedback guarantees uniform ultimate boundedness for uncertian dynamical systems," *IEEE Trans. Automat. Contr.*, vol. AC-26, pp. 1139–1144, 1981.

[67] A. F. Filippov, *Differential Equations with Discontinuous Righthand Sides*. Amsterdam, The Netherlands: Kluwer, 1988.

[68] W. Hahn, *Theory and Application of Liapunov's Direct Method*. Englewood Cliffs, NJ: Prentice-Hall, 1963.

[69] H. K. Khalil, *Nonlinear Systems*. Englewood Cliffs, NJ: Prentice-Hall, 1996.

[70] S. K. Mazumder, A. H. Nayfeh, and D. Boroyevich, "Independent discontinuous control of parallel three-phase boost converters: Solutions and limitations," *IEEE Trans. Power Electron.*, to be published.

[71] F. C. Lee, *Modeling, Analysis, and Design of PWM Converter*. Blacksburg, VA: Virginia Power Electronics Center, 1990.

[72] J. C. Gerdes, "Decoupled design of robust controllers for nonlinear systems: As motivated by and applied to coordinated throttle and brake control for automated highways," Ph.D. dissertation, Dept. Mech. Eng., Univ. California, Berkeley, CA, 1996.

[73] A. A. Stotsky, J. K. Hedrick, and P. P. Yip, "The use of sliding modes to simplify the backstepping control method," *Appl. Math. Computat. Sci.*, vol. 8, no. 1, pp. 123–133.
[74] W. T. McLyman, *Designing Magnetic Components for High-Frequency DC–DC Converters*. New York: K G Magnetics, 1993.

Sudip K. Mazumder (S'01–M'02) received the M.S. degree in electrical power engineering from the Rensselaer Polytechnic Institute (RPI), Troy, NY, in 1993 and the Ph.D. degree in electrical and computer engineering from the Virginia Polytechnic Institute and State University (VPI&SU), Blacksburg, in 2001.

He joined the Center for Power Electronics Systems (NSF Center), VPI&SU, in 1997. Currently, he is an Assistant Professor at the Power Electronics Research Center (PERC), Department of Electrical and Computer Engineering, University of Illinois at Chicago. He has eight years of professional experience in the area of power electronics, motor drives, and motion control. His areas of expertise and interests include distributed power systems: design, modeling and analysis, control (nonlinear and distributed), and integration of power converters, advanced communication protocols, fault-handling schemes; advanced DSP/RISC based embedded controllers for interface to high-performance drives and power structures and communication protocols; multiaxis and multimotor drives and new motor-control algorithms (e.g., variable-structure, H-inf, Lyapunov-based); electric/hybrid vehicle; power quality and voltage sags: parallel converters, active filters, hybrid converters, multilevel converters; renewable energy systems; reliability of converters and power systems; optical switching in power electornics; soft-switching and hard-switching topologies and techniques in power converters; nonlinear dynamics (bifurcation and homotopy theory for nonlinear discontinuous switching systems) and nonlinear control; spatiotemporal modeling for packaging, e.g., for field and thermal distribution, and virtual-reality-based prototyping. He has published 35 international journal and conference papers, two invited papers, and two invention disclosures and a book (in preparation).

Dr. Mazumder received the prize-paper award from the IEEE TRANSACTIONS ON POWER ELECTRONICS and the IEEE Power Electronics Society in 2002. He is listed in *Who's Who in Engineering Education*. He is a member of four IEEE societies and also the Reviewer for eight international journals and conferences. He was the Session Chair for IEEE PESC'01 (Inverter Control Techniques) and the IEEE APEC'02 (Utility Interface and High Power Electronics) Conferences. He is a member of the IAS IDC Program Committee and the Session Organizer for the IAS IDC 2002 Conference.

Ali H. Nayfeh was born in Shuwaikah, Jordan, on December 21, 1933. He received the B.S. degree in engineering science and the M.S. and Ph.D. degrees in aeronautics and astronautics from Stanford University, Stanford, CA, in 1962, 1963, and 1964, respectively.

He has industrial experience with Heliodyne Corporation and Aerotherm Corporation. He is the author of *Perturbation Methods, Introduction to Perturbation Techniques, Problems in Perturbation, Method of Normal Forms* and *Nonlinear Interactions* (New York: Wiley) and coauthor of *Nonlinear Oscillations* and *Applied Nonlinear Dynamics* (New York: Wiley). He is the Editor of the *Wiley Book Series on Nonlinear Science* and the Editor-in-Chief of *Nonlinear Dynamics* and *Journal of Vibration and Control*. He established and served as Dean of the College of Engineering, Yarmouk University, Jordan, from 1980 to 1984. He is currently University Distinguished Professor of Engineering at Virginia Polytechnic Institute and State University.

Dr. Nayfeh received the American Institute of Aeronautics and Astronautics Pendray Aerospace Literature Award in 1995, the American Society of Mechanical Engineers J. P. Den Hartog Award in 1997, the Kuwait Prize in Basic Sciences in 1981, an Honorary Doctorate from St. Petersburg University, Russia in 1996, the Frank J. Maher Award for Excellence in Engineering Education in 1997, the College of Engineering Dean's Award for Excellence in Research in 1998, and an Honorary Doctorate, Technical University of Munchen, Germany, in 1999. He is a Fellow of the American Physical Society, the American Institute of Aeronautics and Astronautics, the American Society of Mechanical Engineers, and the American Academy of Mechanics.

Dushan Borojević (M'90) received the B.S. degree from the University of Belgrade, Yugoslavia, in 1976, the M.S. degree from the University of Novi Sad, Yugoslavia, in 1982, and the Ph.D. degree from Virginia Polytechnic Institute and State University (Virginia Tech), Blacksburg, in 1986.

From 1986 to 1990, he was an Assistant Professor and Director of the Power and Industrial Electronics Research Program, Institute for Power and Electronic Engineering, University of Novi Sad, and later, acting head of the Institute. In 1990, he joined The Bradley Department of Electrical and Computer Engineering, Virginia Tech, as Associate Professor. From 1996 to 1998, he was aAssociate Director of the Virginia Power Electronics Center, and since 1998 he has been the Deputy Director of the NSF Engineering Research Center for Power Electronics Systems and Professor at the Department. His research interests include multiphase power conversion, high-power PWM converters, modeling and control of power converters, applied digital control, and electrical drives. He has published over 100 technical papers, has three patents, and has been involved in numerous government and industry-sponsored projects in the areas of power and industrial electronics.

Dr. Boroyevich is a member of Phi Kappa Phi, the IEEE Power Electronics Society AdCom, IEEE Industry Applications Society Industrial Power Converter Committee.